Time-resolved electronic sum-frequency generation spectroscopy with fluorescence suppression using optical Kerr gating

Caleb J. C. Jordan and Jan R. R. Verlet*

Department of Chemistry, Durham University, Durham, DH1 3LE, United Kingdom

ABSTRACT

Excited state dynamics of molecules at interfaces can be studied using second-order non-linear spectroscopic methods such as time-resolved electronic sum-frequency generation (SFG). However, as such measurements inherently generate very small signals, they are often overwhelmed by signals originating from fluorescence. Here, this limitation is overcome by optical Kerr-gating of the SFG signal to discriminate against fluorescence. The new approach is demonstrated on the excited state dynamics of malachite green at the water/air interface, on it in the presence of a highly fluorescent coumarin dye, and on the photo-oxidation of the phenolate anion at the water/air interface. The generality of the use of optical Kerr gating to SFG measurements is discussed.

* j.r.r.verlet@durham.ac.uk

1. INTRODUCTION

Sum-frequency generation (SFG) is a non-linear optical process that occur under intense electric fields and which relies on the second-order electric susceptibility, $\chi^{(2)}$, of materials. Within the electric dipole approximation, $\chi^{(2)}$ is only non-zero where centrosymmetry is broken and, hence, SFG is restricted to non-centrosymmetric materials and interfaces over the length-scale of the broken symmetry; this is the key property that enables its exploitation as a spectroscopic probe for materials and molecules at interfaces.[1–4] Second harmonic generation (SHG) is a subgroup of SFG (the two driving fields are of equal frequency) and when we discuss SFG, this may also include SHG in certain cases. The interest in SFG as a surface probe has grown over the past few decades[5,6] as interfacial processes are ubiquitous in fields ranging from catalysis to biological and atmospheric chemistry.[7–10] As the need to develop an understanding of chemistry at interfaces increases, so too have the methods to experimentally probe this chemistry. Such methods include the development of time-resolved SFG,[11,12] phase-sensitive SFG,[13–16] heterodyne-detected SFG,[17–19] broadband SFG spectroscopy,[20–23] and 2D SFG.[24] Common to many of these methods is their use of spectral ranges in the UV or IR regions, which each reveal complementary information about the chemical systems they probe. In recent years, there has been a noticeable shift towards the use of vibrational SFG (VSFG) spectroscopy, in which the SFG field at frequency ω_{SFG}, is generated by an IR field that is mixed with a near-IR one (typically 800 nm from a Ti:Sapphire laser).[25,26] The IR spectrum is then encoded through the enhancement of the SFG light when the IR field is resonant with vibrational transitions. VSFG has proven a powerful tool to analyse air-liquid interfaces and especially the nature of the air-water interface.[27–30] Extension to phase-sensitive or heterodyne-detected VSFG (HD-VSFG) provides both the real and imaginary parts of $\chi^{(2)}$, thus offering additional insight into aqueous interfaces. These methods have also been extended to the time-domain, allowing the evolution of photo-induced dynamics of chromophores at aqueous

interfaces to be probed in real time.[31,32] However, by probing the interfacial solvent in such experiments, one does not directly probe the photo-dynamics of the chromophore, which is typically the species of interest. For example, it was recently shown that the dynamics of photoexcited phenol at the water-air interface differs by 4 orders of magnitude compared to similar dynamics bulk water, however, this was inferred from changes in vibrational spectrum of the interfacial water molecules (i.e. the solvation) rather than by probing the evolution of the excited states of phenol or the production of products.[33]

To probe photo-induced dynamics of molecules at interfaces directly, electronic sum-frequency generation (ESFG) can be used. In this case, ω_{SFG} is generated by driving fields in the visible and/or near-UV. Similar to VSFG, it can be easily extended to the time-domain (TR-ESFG) using a pump pulse and delayed probe fields to generate the SFG signal. Indeed, most early studies on the photo-induced dynamics of molecules at interfaces (especially aqueous) were TR-ESFG (or ESHG) experiments.[12,34–37] Similar to VSFG, the ESFG signal can be resonantly enhanced through either driving field or by ω_{SFG} being resonant with an electronic transition in an interfacial chromophore. TR-ESFG can also be extended to be phase-sensitive[38,39] and to heterodyne detection, as demonstrated in a series of impressive experiments by Tahara and coworkers.[31,40] TR-ESFG is highly informative because, in principle, resonance-enhancement of the SFG signal is proportional to the number of molecules on the surface, and hence, it can be used to track interfacial concentrations as a function of time. This is similar in spirit to transient absorption spectroscopy, which has become the workhorse to probe bulk excited state dynamics. Therefore, TR-ESFG has the potential to become a workhorse to track interfacial dynamics.

Despite the potential of ESFG as a general experimental method to probe interfacial photo-induced dynamics, it has experimental hurdles that are often not highlighted. As a $\chi^{(2)}$ process, the SFG signal is generally weak compared to the driving fields. When detecting these weak

signals, such as via photon counting in a simple homodyne-detected ESFG experiment, light generated from the surface that cannot be spectrally separated from ω_{SFG} can result in poor signal-to-noise ratios. A particular issue arises in systems with fluorescent components that overlap with ω_{SFG} in the frequency domain. Phase-sensitive measurements can alleviate this to some extent because of the incoherent nature of fluorescence, but it comes at the expense of increased experimental complexity and there are limits to the extent of fluorescence that can be accommodated. Fluorescence is common and seen in a large fraction of chromophores that are of scientific interest and, because it can arise from the bulk and not just the surface, it generally dwarfs any SFG signal. Although not commonly acknowledged, the general approach to avoid the contribution of fluorescence is to ensure that $\omega_{SFG} > \omega_{pump}$, where ω_{pump} is the frequency of the pump field that induces fluorescence. While effective, this approach is not always applicable because of the high density of states at high energy, so that disentangling the transitions leading to resonance enhancement can be difficult. A potential alternative approach is to exploit the differences in the surface SFG versus fluorescence signals, where the former is coherent, polarised, and temporally short – on the timescale of the duration of the fundamental fields ω_1 and ω_2. As a result, optical methods could, in principle, be exploited to reject the fluorescence, which has previously been demonstrated in a similar fashion for Raman spectroscopy[41] and time-resolved fluorescence spectroscopy.[42–44]

In this study, we offer a simple and effective means to supress fluorescence in a TR-ESFG experiment by using optical gating of the SFG signal. Specifically, we used optical Kerr gating (OKG) as a fast and broadband method. OKG is a common technique in ultrafast time-resolved fluorescence measurements, whereby a temporally long emission signal is gated for measurement in short windows set by an intense gate pulse.[45,46] By scanning the gating window through a response, the entire signal can be built up to observe fluorescence with ~100 fs resolution. OKG relies on an intense gate pulse inducing a change in refractive index in a

material, the Kerr medium (KM), along one axis. When a linearly-polarised 'probe' field is transmitted through the KM without the gate present, its polarisation remains unchanged on propagation. When the gate and probe are incident on the material at the same time, the probe will experience a different refractive index for its polarisation components parallel and perpendicular to the gate, rotating the polarisation of the probe. If the KM is set between two crossed polarisers, then incoming light will not be transmitted unless it is rotated by the gate pulse. Therefore, in the context of surface ESFG, by timing the gate pulse to coincide with the SFG response from the surface, we anticipate that the probe will be transmitted through the KM while the vast majority of the fluorescence emission, which lags the SFG, should be rejected. While TR-ESFG and OKG themselves are not new, the combination of these well-established methods provides a robust method to study excited state processes of molecules at interfaces.

2. EXPERIMENTAL

The general layout of optical components for the time-resolved optical Kerr-gated ESFG (TR-OKG-ESFG) set-up is shown in Figure 1. All laser pulses used were derived from a Yb:KGW laser system (Carbide, Light Conversion) producing 84 µJ, 250 fs pulses at 1028 nm and with a 60 kHz repetition rate. Approximately 30 µJ pulse^{-1} was directed into a 514 nm pumped optical parametric amplifier (OPA) (Orpheus, Light Conversion). For the experiments described here, we used light at 720 nm (signal) with 1.3 µJ pulse^{-1}. This served as one of the SFG driving fields, ω_1. The remainder of the 1028 nm light (~54 µJ pulse^{-1}) was further split using a half-wave plate and polarising beam-splitting optic to produce ~4.1 µJ pulse^{-1} and this beam served as the second of the SFG driving fields, ω_2. The remaining ~50 µJ pulse^{-1} was used to generate pump pulses.

The ω_1 and ω_2 beams were temporally overlapped using a manual delay line in the ω_2 beam line and subsequently combined collinearly and focussed onto the sample surface by a concave mirror (f = 20 cm) at approximately 70° from the surface normal. Both fundamental beams passed through appropriate half-wave plates prior to recombination so their polarisations could be varied independently.

The pump beam was generated by first chopping the 1028 nm pulse train at 30 kHz using a rubidium titanyl phosphate (RTP) crystal (Leysop) and polarising beam splitting optic. This rotated the polarisation of every other pulse in the train by 90° to be reflected and dumped. The remaining 30 kHz train of pulses was converted to its fourth harmonic using two consecutive BBO crystals, resulting in pulses at 257 nm, with ~200 fs duration and up to 3 μJ pulse^{-1}. This was aligned and focussed onto the sample by a concave mirror (f = 20 cm) at approximately 65° from the surface normal. An adjustable time delay, relative to the ω_1 and ω_2 pulses, was controlled by a commercial delay stage (Physik Instumente). The ESFG generated from the surface was collected in reflection geometry and the residual reflected pump was blocked.

Sample solutions were contained in a standard petri dish, rotated at approximately 15 rpm to refresh the sample. The height of the sample surface was monitored and maintained to within ±15 μm. After reflection from the sample surface, the beam containing ω_1, ω_2, and ω_{SFG} (at 423 nm) was recollimated by a plano-convex lens (f = 25 cm) and ω_{SFG} was separated from ω_1 and ω_2 using a Pelin-Brocca prism.

The SFG was directed to the OKG arrangement. This consisted of two perpendicularly polarised Glan-Taylor prisms, between which were two plano-convex lenses (f = 15 cm and f = 5 cm, sequentially) and, at the focus of the telescope, a UV fused silica cuvette with a 1 cm path length containing liquid benzene was placed. At the focus, the ω_{SFG} beam has a diameter

of <100 μm. Benzene was used as a Kerr medium because of its ease of use, good efficiency and suitable response time.

To drive the OKG, residual 1028 nm light from the OPA was used (2.3 μJ pulse^{-1}) and focussed to a diameter of <100 μm by a plano-convex lens (f = 10 cm). The temporal delay between the probe and gate pulses was adjusted manually by a manual translation stage and the polarisation of the gate was set to 45° relative to the ω_{SFG} using a half-waveplate.

The data acquisition involved using a photomultiplier tube (H7732-10, Hamamatsu) to convert ω_{SFG} light into electrical pulses. These were then sent to an amplifier-discriminator (F-100TD, Advanced Research Instruments Corp.), producing short TTL-level pulses above a single-photon threshold. The output pulses were AND-gated with the synchronous output from the driving laser. To perform shot-to-shot background subtraction, the output TTL train was split into two separate 30 kHz channels by in-house electronics, each counted by a multifunction DAQ device (USB-6210, National Instruments).

Experiments were conducted on malachite green, malachite green with coumarin 2, and sodium phenolate. All chemicals were purchased from Sigma Aldrich and used as received. Solutions were made up by dissolving the appropriate amount of chemical in high purity water (Millipore, Milli-Q Gradient A10, 18.2 MΩ). The coumarin dye was dissolved in ethanol. The sodium phenolate solution was made by combining equal parts aqueous phenol and sodium hydroxide solutions.

3. RESULTS

To demonstrate the efficiency of the OKG, results on aqueous malachite green (75 μM) are first considered. Malachite green (MG) has been studied extensively in relation to aqueous surface nonlinear techniques on account of its strong nonlinear response and surface

activity.[36,47–49] The electronic structure of MG is characterised by a strong $S_1 \leftarrow S_0$ transition peaking around 620 nm and a second weaker $S_2 \leftarrow S_0$ transition peaking around 420 nm. Excitation at 257 nm accesses a dense manifold of higher-lying excited states. Hence, ω_1 and ω_2 are not resonant with any transition, but ω_{SFG} is expected to be resonant with the $S_2 \leftarrow S_0$ transition, and this resonance enhancement of the SFG signal is expected to be proportional to the square of the surface concentration.[50] In Figure 2, the square-root of the SFG signal is shown for the dynamics probed over the first 40 ps following excitation. The SFG signal was obtained in PPP polarisation configuration. The black trace shows the results when no OKG was applied and the polarisers were set parallel to allow all light to pass. The signal at $t < 0$ arises from SFG generated by the resonance-enhancement with the $S_2 \leftarrow S_0$ transition. At $t = 0$, some population is transferred to higher-lying excited states, which reduces the concentration of molecules in the S_0 state and, hence, reduces the SFG generated. The observed partial recovery shows that some population returns to S_0. The timescale and overall dynamics are in excellent agreement with previous TR-SHG studies,[48,51] including those from our group in which malachite green was excited at 250 nm and probed by 800 nm pulses with the SHG at 400 nm. The second, blue trace shows the results of an experiment in which the OKG was operated and the two polarisers we set perpendicular to each other. The overall dynamics appear similar although there is a small overall reduction in signal. To directly compare the two traces, in Figure 2(b), the difference in the square-root of the SFG signal is shown in which signal from $t < 0$ has been subtracted to leave only the dynamical changes.

As seen clearly in Figure 2(b), the overall appearance of the kinetics is unaffected (as expected). The small differences in amplitude arise from small changes in alignment required when rotating one of the polarisers. From direct measurements of the photomultiplier output seen from the square root of signals before t_0 in Figure 2(a), we determine that the efficiency

of the OKG is approximately 75%. Note that each time-resolved trace in Figure 2 required only 5 minutes of data acquisition.

The inset in Figure 2(b) shows the temporal resolution of the OKG. This was measured by operating the OKG set to achieve maximal transmission of a ω_{SFG} pulse generated in a BBO crystal above the surface as a function of delay between the gate and the ω_{SFG} pulses and then scanning the delay and optimising the overlap between the gate pulse and the ω_{SFG} pulse. The inset of Figure 2(b) clearly demonstrates that the ω_{SFG} pulse is only observable in the presence of the gate. The overall response of the transmission closely follows that documented previously for benzene, which predominantly displays a Gaussian, electronic response, with a visible asymmetry over a few picoseconds resulting from the slower, nuclear response of the liquid.[45,52]

Figure 2(a) and (b) provide a demonstration of the function of OKG and its efficiency. However, malachite green, does not exhibit much fluorescence, even when pumped at 257 nm. To test the impact of a fluorophore, a highly fluorescent dye molecule was added to the malachite green solution. Specifically, the addition of Coumarin 2 will lead to strong fluorescence at 420 nm and may be expected to saturate the photon counter. To enable this measurement, we reduced the intensity of the ω_2 field, and by extension that of ω_{SFG}, so as to simulate a more characteristic strength of surface response. It must also be noted that the pump intensity was decreased for this measurement, as otherwise the surface fluorescence alone was enough to saturate the pump-on counter. Without the addition of OKG, the fluorescence from the sample is much greater than that of the SFG signal from MG, and even the relatively large signal from MG is obscured by the fluorescence when photon counting in this regime. However, the fluorescence occurs over much longer timescales than the SFG signal, and by aligning the OKG with the SFG pulse, the vast majority of the photons generated by fluorescence, which will lag the SFG by a range of time up to nanoseconds, can be suppressed.

This is shown in Figure 2(c), where the ungated signal (black trace) is virtually featureless, whereas the OKG signal (blue trace) shows a distinct change after t_0, albeit with reduced signal-to-noise on account of the reduced pump and ω_{SFG} intensities. These traces also comprise a single scan (0.5 s acquisition time per data point) for comparison. Even in this extreme case of very strong fluorescence, application of the OKG allows the TR-ESFG signals to be acquired.

Finally, the utility of OKG applied to surface TR-ESFG spectroscopy is supported by measurements on the phenolate anion. Phenol and its anion have been studied previously by SHG and SFG.[33,53,54] Additionally, the photo-induced dynamics have been monitored in the bulk by transient absorption[55,56] and very recently at the surface using TR-HD-VSFG for phenol. It has been shown in bulk solution that excitation of phenolate into the S_1 state at 257 nm will produce hydrated electrons and phenoxy radicals, the former of which is resonant with ω_1. Thus, following excitation, the SFG signal is expected to increase, with signal components that are approximately proportional to the square of the concentrations of hydrated electrons at the surface. At 0.1 M bulk concentration, despite a low quantum yield of 0.007 in aqueous solution,[57] the fluorescence from the phenolate molecules was large compared to the SFG response, completely saturating the photon counter and preventing observation of the interfacial kinetics. At reduced pump intensities and without OKG, the surface signal is too weak to be detected. Hence, the need for some form of discrimination against fluorescence is clearly highlighted in this system.

Figure 3 shows the results of TR-OKG-ESFG of the phenolate anion at the water/air interface following excitation at 257 nm (with SFG acquired in the PPP configuration). By applying OKG to the SFG signal, the fluorescence can be effectively removed from the detected signal. The data in Figure 3 is an average of two scans, equating to 15 minutes of data acquisition. The positive signal at $t > 0$ indicates an increased concentration of hydrated electrons following pump excitation at the aqueous surface. The signal rises to a maximum at

~2.5 ps and subsequently decays on a timescale of approximately 20 ps, leaving a long-lived offset at later times. Similar overall dynamics have been observed in the bulk, albeit with slightly different timescales. The initial rise in signal was associated with the formation of a contact pair of the phenoxy-radical and a solvated electron. The subsequent decay was assigned to a competition between geminate recombination to reform the phenolate anion and dissociation of the contact pair to form free hydrated electrons. The latter can then be assigned to the observed offset at long times. This subsequently decays in the bulk due to diffusion of the phenoxy radical and hydrated electron that can subsequently recombine. The overall similarity between bulk and interfacial dynamics suggests that a very similar process is taking place at the surface, although subtly different solvation environments might affect the lifetimes.[39,58] This will be investigated in detail in a later study.

To estimate the efficiency of fluorescence rejection by the Kerr gating, we monitored the photon count rate with no probe pulses (ω_1 or ω_2) present. In the presence of only pump pulses and with the OKG operating, the maximum photon count rate was 1.3×10^{-4} counts pulse^{-1}. With gate polarisers parallel, the OKG gate pulse blocked, and the light attenuated to 10% transmission (using a OD1 neutral density filter), the maximum photon count rate was 0.4 counts pulse^{-1}. From this, we estimate that the Kerr gate transmits less than one in every 30,000 fluorescence photons for phenolate pumped at 257 nm.

4. DISCUSSION AND CONCLUSION

OKG has the potential to be widely applicable to many surface SFG setups: it is simple to incorporate provided a sufficiently intense gate pulse can be supplied to facilitate a high gating efficiency. The technique can also be used in phase-sensitive SFG experiment that make use of spatial interference or phase-delay methods, where transmission of a single interfering signal

pulse through the gate is straightforward. Conversely, OKG may be less suited for heterodyne-detected methods in which the local oscillator and SFG fields are separated by a few picoseconds in time to generate a spectral interferogram, unless the OKG gate can be opened for a sufficient time (at the expense of increased fluorescence contributions). Kerr gating is not wavelength specific and is therefore pertinent to broadband ESFG and ESHG, enabling its application to many existing techniques. OKG is a well-established technique that has a broad range of literature on the behaviours of different materials used as a KM for different applications. By combining SFG techniques and OKG in detection, a large range of interesting surface-active compounds can be made accessible for surface nonlinear spectroscopy that may previously have been considered off-limits.

Acknowledgements

We are grateful to Prof. Andy Beeby for many useful discussions concerning OKG and the loan of Glan-Taylor prisms. CJCJ was supported by the ESPRC Doctoral Training Partnership (EP/R513039/1).

Data Availability Statement

The data that support the findings of this study are available from the corresponding author upon reasonable request.

References

[1] N. Bloembergen and P.S. Pershan, Phys. Rev. **128**, 606 (1962).

[2] P. Guyot-Sionnest, W. Chen, and Y.R. Shen, Phys. Rev. B **33**, 8254 (1986).

[3] Y.R. Shen, *Principles of Nonlinear Optics* (2002).

[4] Y.R. Shen, Nature **337**, 519 (1989).

[5] G.L. Richmond, Chem. Rev. **102**, 2693 (2002).

[6] K.B. Eisenthal, Chem. Rev. **96**, 1343 (1996).

[7] C. George, M. Ammann, B. D'Anna, D.J. Donaldson, and S.A. Nizkorodov, Chem. Rev. **115**, 4218 (2015).

[8] C.T. Williams and D.A. Beattie, Surf. Sci. **500**, 545 (2002).

[9] O. Björneholm, M.H. Hansen, A. Hodgson, L.-M. Liu, D.T. Limmer, A. Michaelides, P. Pedevilla, J. Rossmeisl, H. Shen, G. Tocci, E. Tyrode, M.-M. Walz, J. Werner, and H. Bluhm, Chem. Rev. **116**, 7698 (2016).

[10] S. Yang, H. Noguchi, and K. Uosaki, J. Phys. Chem. C **122**, 8191 (2018).

[11] Y. Rao, D. Song, N.J. Turro, and K.B. Eisenthal, J. Phys. Chem. B **112**, 13572 (2008).

[12] A. Castro, E. V. Sitzmann, D. Zhang, and K.B. Eisenthal, J. Phys. Chem. **95**, 6752 (1991).

[13] R.K. Chang, J. Ducuing, and N. Bloembergen, Phys. Rev. Lett. **15**, 6 (1965).

[14] R. Superfine, J.Y. Huang, and Y.R. Shen, Opt. Lett. **15**, 1276 (1990).

[15] K. Kemnitz, K. Bhattacharyya, J.M. Hicks, G.R. Pinto, B. Eisenthal, and T.F. Heinz, Chem. Phys. Lett. **131**, 285 (1986).

[16] R. Stolle, G. Marowsky, E. Schwarzberg, and G. Berkovic, Appl. Phys. B Lasers Opt. **63**, 491 (1996).

[17] I. V. Stiopkin, H.D. Jayathilake, A.N. Bordenyuk, and A. V. Benderskii, J. Am. Chem. Soc.

130, 2271 (2008).

[18] S. Yamaguchi and T. Tahara, J. Chem. Phys. **129**, 101102 (2008).

[19] S. Sun, R. Liang, X. Xu, H. Zhu, Y.R. Shen, and C. Tian, J. Chem. Phys. **144**, 244711 (2016).

[20] J.A. McGuire, W. Beck, X. Wei, and Y.R. Shen, Opt. Lett. **24**, 1877 (1999).

[21] E.W.M. van der Ham, Q.H.F. Vrehen, and E.R. Eliel, Opt. Lett. **21**, 1448 (1996).

[22] L.J. Richter, T.P. Petralli-Mallow, and J.C. Stephenson, Opt. Lett. **23**, 1594 (1998).

[23] K. Sekiguchi, S. Yamaguchi, and T. Tahara, J. Chem. Phys. **128**, 114715 (2008).

[24] W. Xiong, J.E. Laaser, R.D. Mehlenbacher, and M.T. Zanni, Proc. Natl. Acad. Sci. U. S. A. **108**, 20902 (2011).

[25] X.D. Zhu, H. Suhr, and Y.R. Shen, Phys. Rev. B **35**, 3047 (1987).

[26] S. Yamaguchi and T. Otosu, Phys. Chem. Chem. Phys. **23**, 18253 (2021).

[27] M. Vinaykin and A. V. Benderskii, J. Phys. Chem. Lett. **3**, 3348 (2012).

[28] N. Ji, V. Ostroverkhov, C.S. Tian, and Y.R. Shen, Phys. Rev. Lett. **100**, 096102 (2008).

[29] C.S. Tian and Y.R. Shen, J. Am. Chem. Soc. **131**, 2790 (2009).

[30] S. Nihonyanagi, R. Kusaka, K.I. Inoue, A. Adhikari, S. Yamaguchi, and T. Tahara, J. Chem. Phys. **143**, 124707 (2015).

[31] K. Matsuzaki, R. Kusaka, S. Nihonyanagi, S. Yamaguchi, T. Nagata, and T. Tahara, J. Am. Chem. Soc. **138**, 7551 (2016).

[32] K. Inoue, T. Ishiyama, S. Nihonyanagi, S. Yamaguchi, A. Morita, and T. Tahara, J. Phys. Chem. Lett. **7**, 1811 (2016).

[33] R. Kusaka, S. Nihonyanagi, and T. Tahara, Nat. Chem. **13**, 306 (2021).

[34] R. Antoine, A.A. Tamburello-Luca, P. Hébert, P.F. Brevet, and H.H. Girault, Chem. Phys. Lett. **288**, 138 (1998).

[35] D. Zimdars, J.I. Dadap, K.B. Eisenthal, and T.F. Heinz, J. Phys. Chem. B **103**, 3425 (1999).

[36] X. Shi, E. Borguet, A.N. Tarnovsky, and K.B. Eisenthal, Chem. Phys. **205**, 167 (1996).

[37] J.A. McGuire and Y.R. Shen, Science **313**, 1945 (2006).

[38] A.L. Tyson, D.A. Woods, and J.R.R. Verlet, J. Chem. Phys. **149**, 204201 (2018).

[39] P.J. Nowakowski, D.A. Woods, and J.R.R. Verlet, J. Phys. Chem. Lett. **7**, 4079 (2016).

[40] S. Yamaguchi and T. Tahara, J. Phys. Chem. C **119**, 14815 (2015).

[41] P. Matousek, M. Towrie, C. Ma, W.M. Kwok, D. Phillips, W.T. Toner, and A.W. Parker, J. Raman Spectrosc. **32**, 983 (2001).

[42] J. Takeda, K. Nakajima, S. Kurita, S. Tomimoto, S. Saito, and T. Suemoto, Phys. Rev. B - Condens. Matter Mater. Phys. **62**, 10083 (2000).

[43] H. Lemmetyinen, N. V. Tkachenko, B. Valeur, J. Hotta, M. Ameloot, N.P. Ernsting, T. Gustavsson, and N. Boens, Pure Appl. Chem. **86**, 1969 (2014).

[44] T. Fujino, T. Fujima, and T. Tahara, Appl. Phys. Lett. **87**, 131105 (2005).

[45] S. Arzhantsev and M. Maroncelli, Appl. Spectrosc. **59**, 206 (2005).

[46] K. Appavoo and M.Y. Sfeir, Rev. Sci. Instrum. **85**, 055114 (2014).

[47] P. Fita, A. Punzi, and E. Vauthey, J. Phys. Chem. C **113**, 20705 (2009).

[48] P.J. Nowakowski, D.A. Woods, C.D. Bain, and J.R.R. Verlet, J. Chem. Phys. **142**, 084201 (2015).

[49] A. Punzi, G. Martin-Gassin, J. Grilj, and E. Vauthey, J. Phys. Chem. C **113**, 11822 (2009).

[50] J.M. Hicks, K. Kemnitz, K.B. Eisenthal, and T.F. Heinz, J. Phys. Chem. **90**, 560 (1986).

[51] Pratik Sen, Shoichi Yamaguchi, and Tahei Tahara, Faraday Discuss. **145**, 411 (2010).

[52] Y. Wang, L. Sui, Y. Jiang, D. Liu, Q. Li, A. Chen, and M. Jin, Fourth Int. Symp. Laser Interact. with Matter **10173**, 101731Y (2017).

[53] A.A. Tamburello-Luca, P. Hébert, P.F. Brevet, and H.H. Girault, J. Chem. Soc. - Faraday Trans. **92**, 3079 (1996).

[54] R. Kusaka, T. Ishiyama, S. Nihonyanagi, A. Morita, and T. Tahara, Phys. Chem. Chem. Phys. **20**, 3002 (2018).

[55] A.L. Tyson and J.R.R. Verlet, J. Phys. Chem. B **123**, 2373 (2019).

[56] X. Chen, D.S. Larsen, S.E. Bradforth, and I.H.M. Van Stokkum, J. Phys. Chem. A **115**, 3807 (2011).

[57] N. Getoff, Int. J. Radiat. Appl. Instrumentation. Part **34**, 711 (1989).

[58] D.M. Sagar, C.D. Bain, and J.R.R. Verlet, J. Am. Chem. Soc. **132**, 6917 (2010).

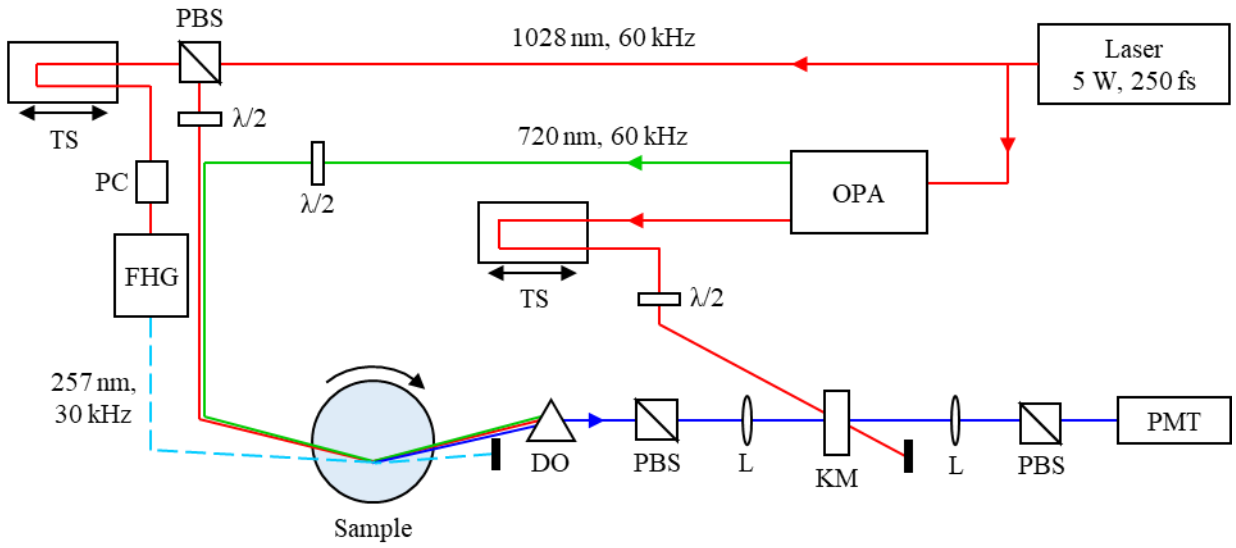

Figure 1: Simplified schematic of experimental setup. PBS = polarising beam splitter, λ/2 = half-wave plate, TS = translation stage, PC = Pockels cell, FHG = fourth harmonic generation, DO = dispersing optic (Pelin Brocca prism), L = lens, KM = Kerr medium, PMT = photo-multiplier tube. Collinear beams are visually offset for clarity.

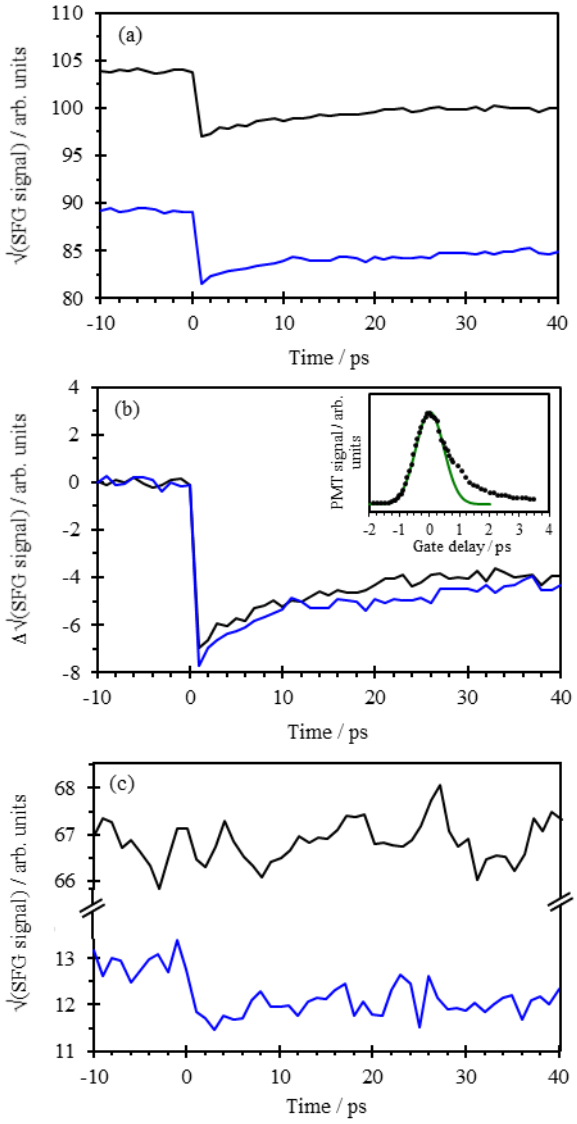

Figure 2: (a) Transient surface SFG signal (PPP) recorded from aqueous MG without OKG (black) and with OKG (blue). (b) Background-subtracted traces of the same data in (a). Inset shows efficiency of the Kerr gate as a function of delay between the gate and SFG pulses (dots) with Gaussian fit (green line). Positive gate delay indicates the SFG pulse arrives after the gate. (c) Transient surface SFG signal (PPP) recorded from aqueous MG without OKG (black) and with OKG (blue), in the presence of coumarin 2.

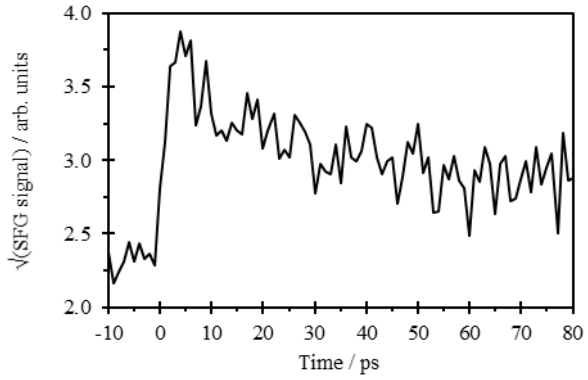

Figure 3: Transient surface SFG signal (PPP) recorded from 0.1 M aqueous sodium phenolate with OKG.